A Comparison of Joint Control Algorithms for Teleoperated Pick and Place Tasks Using a Flexible Manipulator

Lonnie J. Love David P. Magee Wayne J. Book
The George Woodruff School of Mechanical Engineering
Georgia Institute of Technology
Atlanta, GA 30332-0405

Abstract

This paper presents initial results of an on going study of robot control algorithms used for teleoperation of long reach manipulators. The focus of the paper is the effect of the slave robot control algorithm on the performance of a teleoperation schemes that uses long reach, flexible manipulators. This study investigates the influence of PD , PD with input shaping, and PD with modified command filtering on pick and place teleoperation tasks.

Data from 90 trials using 6 operators is used in an attempt to identify any increase in performance resulting from the use of any of the above control schemes. The results of this investigation indicate an increase in performance, based upon a combination of interaction forces and task execution time, of teleoperated pick and place tasks when a flexible robot uses either PD with input shaping or PD with modified command filtering.

Introduction

In 1991, the United States Department of Energy committed to a 30-year program to retrieve, characterize, package, and dispose of the nuclear waste resulting from 40-years of nuclear weapons' production [1]. From 1949 to 1964, 149 single-shell tanks (SST) were constructed in Hanford, Washington for the long term storage of nuclear waste generated by the construction of nuclear weapons.

The nuclear waste sites were designed for long term storage of large quantities of hazardous materials. These carbon-steel-lined, concrete reinforced tanks have held waste for 40 years and some are known to leak. No provisions were made to enable the extraction of the stored materials. A variety of ideas have been considered which range from cutting into the tanks to using self-propelled vehicles to deploy tooling within the SST. Many tanks are approximately 75 feet in diameter and 29 to 45 feet in depth. The only designed access is through a 42-inch diameter access port at the top of the tanks [2]. The consistency of materials inside the tanks ranges from liquid and sludge to saltcakes as hard as concrete. Hardware installed in the tanks for monitoring and previous operations further complicate removal of the contents. Due to the size and nature of the problem, the use of long reach robotics may prove to be one viable approach [3].

Long Reach Manipulators

The small access and large workspace of the tanks force the use of long slender arms on the manipulators performing cleanup operations. The characteristics associated with these arms are reduced weight and large workspace, but increased compliance. This compliance has been a topic of active research for the past 20 years at Georgia Tech. One long reach manipulator at Georgia Tech, RALF (Robotic Arm Large and Flexible) illustrated in Figure 1, is a planar 2 DOF elastic manipulator. It consists of two cylindrical links with a span of 10 feet each and has a payload capacity of 60 lbs. with a structural weight of 100 lb.

Command Filtering

Most elastic robot control schemes focus on accurate position or motion tracking of the tip [4]. Many of these techniques produce desirable performance but require precise knowledge of the robot's dynamics [5]. In addition, many control schemes require precomputed trajectories for the robot to follow. Tasks that require teleoperation are generally unstructured and cannot be modelled in advance. Techniques that use path planning are therefore not admissible for teleoperation schemes. As a manipulator maneuvers around a workspace and manipulates objects, the dynamics associated with the robot vary. With elastic manipulators, these variations can produce large vibrations in the flexible arms that can lead to instability. Some researchers are investigating methods that modify the commands to the robot actuators and reduce the excitation of the modes of vibration associated with the robot.

The input shaping method was introduced by Singer and Seering [6] as a means of cancelling vibration in systems that are modelled as linear, time-invariant and second-order. Their method relies on linear superposition of the system impulse response so that the net vibration is zero. Their idea suggests delaying a portion of the commanded input by half the damped natural period of the system to cancel the vibration generated by the original input. They also developed a set of non-linear, trigonometric constraint equations that must be solved to determine their input shaping parameters.

Magee and Book [7] extended the idea to a modified command filtering technique that adapts to parameter variation when a system changes configuration. Their algorithm alters the number of terms in the filter so that a uniform output is maintained even when the system parameters change. The filtering technique was able to accommodate the parameter variation throughout the entire workspace of a large flexible manipulator, RALF, while the input shaping method was limited to about a 10% variation. They also showed that the input shaping method takes an iterative form and therefore the set of nonlinear equations do not have to be solved.

In this paper, the three controllers under investigation are PD, PD with input shaping and PD with modified command filtering. The PD algorithm operates on the joint feedback error and was tuned to give a quick and stable response to teleoperated commands. For each of the shaping techniques, the feedback error term was first transformed using a 4 term filter to produce a new shaped error signal. This new error signal was then used in the PD controller to compute a command signal that positions the slave manipulator. Note that the same PD gains were used for all of the controllers.

Teleoperator and the Environment

The teleoperation platform at Georgia Tech consists of a pair of planar, 2 DOF manipulators. The slave robot, RALF, is controlled by a Motorola MC68040 CPU board located in a VME chassis. Two 16 channel A/D boards and two 8 channel D/A boards are used for analog data acquisition and control. The operating system, VxWorks, provides the real-time development system and debugging facility.

The operator views the motion of RALF on two monitors that display black and white camera views of the slave robot's workspace. The first camera records a 20' x 15' vertical plane of motion from the side with a line of sight perpendicular to that plane. A 25" diagonal monitor displays this plane of motion. The second camera can be seen in Figure 3 riding on the second link of RALF and records the immediate vicinity of the gripper. It is used for final positioning before payload pickup and drop-off. A 9" diagonal monitor displays roughly a 14" x 10" rectangle in the plane of the gripper. Contrast between key parts of the payload and task board have been enhanced and background panels have been added to minimize the clutter in the background as a factor in the experiment.

A variety of sensors assist in the control and analysis of RALF. For joint feedback, LVDTs are located at the hydraulic cylinders that drive the robot's joints. A combination of strain gages and lateral effect photo diodes, not used for this study, provide an estimation of each link's deformation. In addition, a landmark based vision system could also be used to measure the endpoint position. A 3 DOF force transducer is located at the tip RALF to provide an estimation of the magnitude and direction of the external forces applied at the tip of the robot.

A second manipulator, HURBIRT (HUman Robot Bilateral Research Tool) illustrated in Figure 2, serves as the master robot for the teleoperation scheme. A DSP based computer (TI TMS320C25) is used to compute the control for the master manipulator. This robot's controller consists of an impedance control algorithm that attempts to compensate for the robot's natural dynamics and produce a desired dynamic response to human commanded forces [8]. The target impedance for the teleoperation scheme effectively produces a response that represents a 2 kg. mass, without gravity, moving through a light viscous fluid. The selection of desired mass and viscous damping produce an indirect method of controlling or limiting the commanded velocity and acceleration from the operator. In addition, a virtual wall that simulates the limits of the slave robot's workspace is superimposed on the master robot's target impedance. These virtual walls constrain the human from commanding the slave to move outside its workspace.

To facilitate the teleoperation tasks, the controller for HURBIRT computes its tip position and scales the position from the space of the master robot to the space of the slave, RALF. Currently, a 7:1 position amplification permits comfortable mapping of RALF's full workspace into the workspace of the human operator. Once the desired tip position for RALF is calculated, the desired joint position is computed and then transmitted to the VME bus for input to the slave controller. Currently, data is transmitted every 5 ms at 38,400 baud using a serial communication port.

To isolate the human operator from the slave environment, the master and slave robots are located in different labs in the same building. This configuration allows the investigators to control the visual, acoustical, and tactile information that the operator might experience. In the specifications for the nuclear waste restoration project, the operator may be located miles from the contamination site. Our testbed attempts to simulate this real world scenario and provide further insight into the human noncollocation problem.

A modular scaffold next to the slave robot permits simple modifications to the slave manipulator's workspace and tasks. Preliminary experiments illustrate that the use of flexible manipulators may be advantageous when performing work on the environment. Interaction forces between rigid robots and stiff environments grow quite rapidly when a robot impedes upon a surface. An elastic robot will deform and accommodate interaction forces when interacting with a rigid environment. Figure 3 illustrates the execution of a pick and place task using RALF and the scaffold.

Experimental Test Procedure

The task investigated in this survey consists of remotely moving a payload between a series of holding stations. All operators performed the same task for all of the experiments. The payload mass used in the pick and place experiments was 6.8 kg. The holding stations, attached to the scaffold in Figure 1, are in a triangular pattern separated by 0.7 m, 2.4 m, and 2.9

m. The tolerance for picking up the payload is 0.01 m.

The teleoperation task consists of:

1) starting with the payload in an initial holding station and the slave manipulator in it's home position
2) moving the slave manipulator to the holding station and picking up the payload
3) relocating the payload to the next holding station
4) returning the slave manipulator to it's home position

This procedure was followed until the payload was returned to it's original holding station.

Six male operators between the ages of 22 to 47 trained for approximately 20 minutes on the teleoperation system using either the PD, PD with input shaping, or PD with modified command filtering. During the execution of the teleoperation task, both the Completion Time (CT) and the force at the tip of RALF were recorded. After the training session, a given operator repeats the teleoperation task using the same control scheme until the variance of his CT converges to a steady state value. Once the variation stabilizes, five additional operations are performed. This procedure attempts to eliminate the effect of the learning process of the teleoperation task used in this study. The operator repeats the same procedure for each of the controllers without knowledge of what scheme is being used to position the slave manipulator. To minimize any bias related to the learning process, the order in which the controllers were used varied from operator to operator.

Statistical Evaluation of Data

Table 1 shows the results for the six operators using the three different controllers and the order in which the controllers were given. The CT is defined as the amount of time required for an operator to perform the payload positioning task discussed earlier. By averaging all of the CTs for a given operator and controller, the mean CT can be computed. A similar statistical analysis was performed on the sampled force data. The standard deviation is also included in Table 1 for each of the various mean calculations. This calculation gives a measure of how the data is distributed for each operator.

To characterize the data between all of the operators and controllers, an overall mean CT and overall mean force were computed. They are defined as the mean of all CTs and the mean of all forces recorded during the study, respectively. A performance index is based upon these calculations and can be defined as

$$Perf.\ Index = \frac{Mean\ CT}{Overall\ Mean\ CT} + \frac{Mean\ Force}{Overall\ Mean\ Force}$$

It is evident that the operator is rewarded for short CTs and for small interaction forces. Thus the lower the performance index, the better. The performance index for all of the operators and controllers is listed in Table 2.

Results and Discussion

The mean CT for all of the tasks performed by all of the operators was 108 seconds. Likewise, the mean interaction force was 64.5 N. Figure 4 is a plot of the tip force magnitude measured from operator 5's last execution of each controller. This figure shows the decrease in the CT associated with each controller as well as the forces during initial contact with and relocation of the payload.

Table 2 shows the normalized CT, the normalized mean force, and the performance index associated with each operator and controller. There is some correlation between the normalized CT and the order in which the controller was administered. As an example, operators 2 and 6 performed the task using modified command filtering first. In both cases, PD alone outperformed PD with modified command filtering. Likewise, operators 3 and 5 performed the task using PD with input shaping first. Again, PD alone outperformed the combined control method. It appears that more learning occurred after the first controller was administered.

Figure 5 and 6 illustrate the scatter of the completion time and performance index for each of the controllers used in this study. The PD controller averaged an index of 2.08 while the addition of input shaping and modified command filtering produced mean indices of 1.99 and 1.93, respectively. Although the scattering associated with the CT did not reveal any clear differences between control methods, the scattering associated with the performance index indicates a distinct trend. First, the mean of the performance index decreased with the addition of input shaping. The mean of the index was further reduced when the modified command filtering was used. Second, the distribution of the index decreased when input shaping was incorporated into the PD controller. The addition of modified command filtering to the PD controller generated an even smaller distribution of the index.

Conclusion

It is difficult to draw any solid conclusions from the results due to the high variance in the data, but trends indicate that some form of trajectory or command filtering should increase the performance in teleoperated pick and place tasks using long reach, flexible manipulators. The authors feel that future operators should have longer periods of acclimation to the system before the learning process is complete. Future research will focus on different types of tasks required in the nuclear waste restoration project. These include teleoperated mechanical assembly, cutting processes, constrained manipulation and disturbance rejection.

Acknowledgement

The authors wish to acknowledge the contribution of time and effort provided by the individuals who participated in this study. This research was sponsored in part by Sandia National Laboratories with the cooperation of Pacific Northwest Laboratories under Contract No. 18-4379G.

References

1. R.Schilling, "Telerobots in the Nuclear Industry: A Manufacturer's View," Industrial Robot. Vol.19, No.2, pp.3-14 (1992).

2. K.L. Morris, A.F. Shattuck, and W.A. Covert, "Selected In-Tank Property Measurement Methods for Hanford Site Single-Shell Tanks." American Nuclear Society 1990 Winter Annual Meeting, Washington, D.C., Nov.11-16, 1990.

3. S.A.Kreig, W.W.Jenkins, K.J.Leist, K.G.Squires, and J.F.Thompson, "Single-Shell Tank Waste Retrieval Study." Westinghouse Hanford Co. Report for the U.S. Dept. of Energy, June 1990.

4. D.P. Magee and W.J. Book, "Control and Control Theory for Flexible Robots." Journal of the Society of Instrument and Control Eng., Vol.32, No.4, pp.309-317, April, 1993.

5. E. Bayo, R. Movagher, and M. Medus, "Inverse Dynamics of a Single-Link Flexible Robot: Analytical and Experimental Results," Int. Journal of Robotics and Automation. Vol.3, No.3, Fall 1988.

6. N.C. Singer and W.P. Seering, *Preshaping Command Inputs to Reduce System Vibration*, Artificial Intelligence Memo No. 1027, Massachusetts Institute of Technology, January, 1988.

7. D.P. Magee and W.J. Book, "Implementing Modified Command Filtering to Eliminate Multiple Modes of Vibration," Proc. of the 1993 American Control Conf., Vol.3, pp.2700-2704, June 2-4, 1993.

8. N.Hogan, "Impedance Control: An Approach to Manipulation: Part I - Theory," ASME Journal of Dyn. Syst., Meas., and Cont., Vol. 107, No.1, pp. 1-24, March 1985.

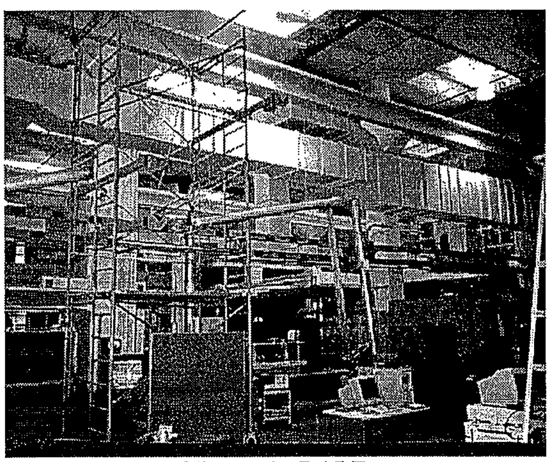

Figure 1: RALF

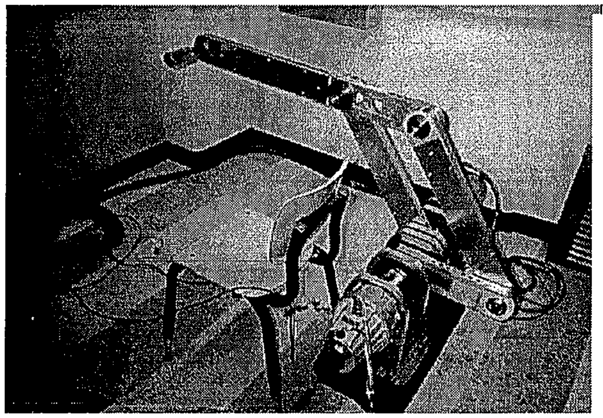

Figure 2: HURBIRT

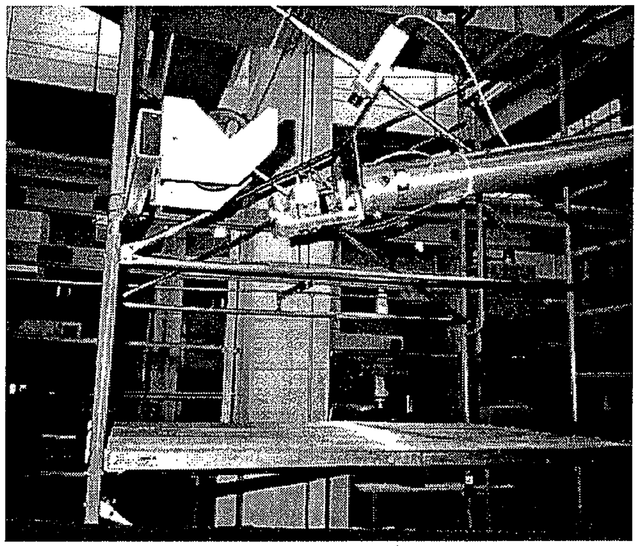

Figure 3: Gripper at the tip of RALF

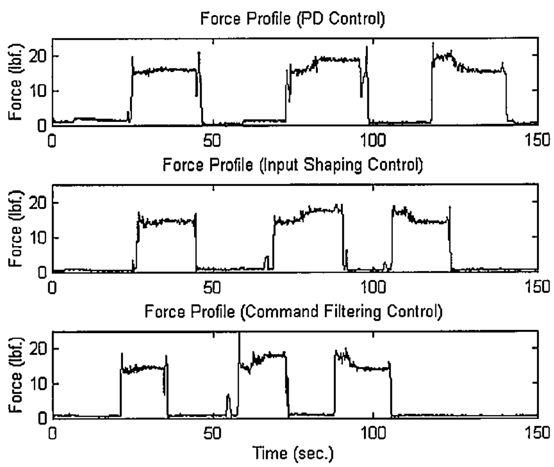

Figure 4: Force Profiles

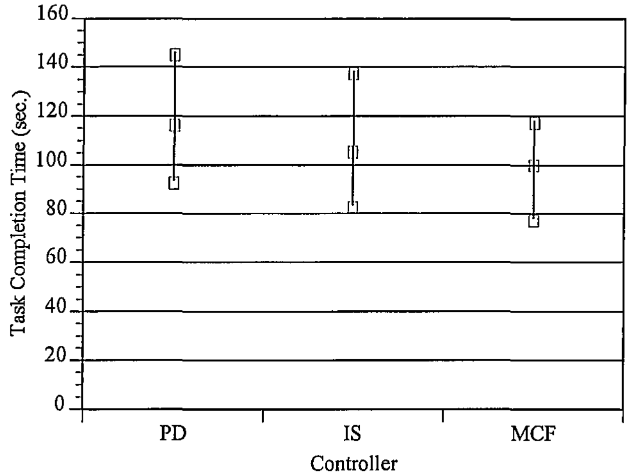

Figure 5: Scatter of Completion Time vs. Controller

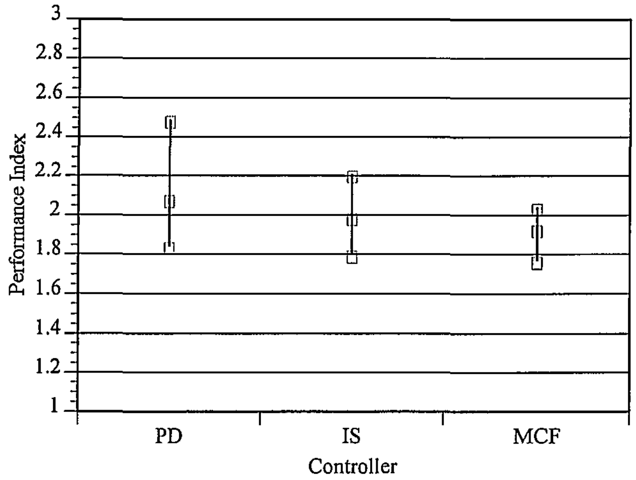

Figure 6: Scatter of Performance vs. Controller

Operator	Controller (order)	Mean CT (St. Dev) (sec)	Mean Peak Force(St. Dev) (N)	Mean Force (St. Dev) (N)
1	PD (1st) input shaping (3rd) command filtering (2nd)	146 (8.3) 112 (4.5) 107 (8.0)	108.1 (18.2) 111.0 (12.0) 104.1 (15.1)	73.4 (0.4) 69.4 (1.3) 67.2 (1.8)
2	PD (3rd) input shaping (2nd) command filtering (1st)	108 (2.9) 100 (6.6) 111 (6.8)	98.7 (15.1) 111.0 (12.4) 97.8 (12.0)	68.9 (1.3) 68.1 (0.9) 65.4 (0.4)
3	PD (2nd) input shaping (1st) command filtering (3rd)	93 (2.1) 103 (5.5) 79 (0.9)	97.4 (13.8) 154.3 (43.1) 111.6 (25.3)	65.4 (1.3) 67.2 (3.1) 67.2 (10.7)
4	PD (1st) input shaping (2nd) command filtering (3rd)	116 (18.0) 83 (4.6) 78 (4.4)	108.5 (28.9) 117.9 (48.0) 106.3 (10.7)	66.7 (8.4) 66.3 (9.3) 76.5 (1.3)
5	PD (3rd) input shaping (1st) command filtering (2nd)	124 (4.0) 138 (5.9) 111 (4.1)	84.1 (10.7) 83.6 (14.7) 80.9 (5.3)	62.7 (0.9) 60.0 (0.9) 61.4 (1.3)
6	PD (2nd) input shaping (3rd) command filtering (1st)	116 (2.8) 101 (2.4) 118 (2.3)	76.5 (19.1) 84.1 (13.8) 72.1 (8.0)	49.4 (1.8) 57.4 (10.2) 48.9 (0.4)

Table 1: Task Completion Time and Force Information

Operator	Controller (order)	Normalized CT	Normalized Mean Force	Performance Index
1	PD (1st) input shaping (3rd) command filtering (2nd)	1.35 1.04 0.99	1.14 1.08 1.04	2.49 2.12 2.03
2	PD (3rd) input shaping (2nd) command filtering (1st)	1.00 0.93 1.03	1.07 1.05 1.01	2.07 1.98 2.04
3	PD (2nd) input shaping (1st) command filtering (3rd)	0.86 0.95 0.73	1.01 1.04 1.04	1.87 1.99 1.77
4	PD (1st) input shaping (2nd) command filtering (3rd)	1.07 0.77 0.72	1.03 1.03 1.19	2.10 1.80 1.91
5	PD (3rd) input shaping (1st) command filtering (2nd)	1.15 1.28 1.03	0.97 0.93 0.95	2.12 2.21 1.98
6	PD (2nd) input shaping (3rd) command filtering (1st)	1.07 0.96 1.09	0.77 0.89 0.76	1.84 1.85 1.85

Table 2: Performance Index